High-Efficiency Electroluminescence from New Blue-Emitting Oligoquinolines Bearing Pyrenyl or Triphenyl Endgroups

Jessica M. Hancock, Angela P. Gifford, Christopher J. Tonzola, and Samson A. Jenekhe*

Departments of Chemical Engineering and Chemistry, University of Washington, Seattle, Washington 98195-1750

Received: December 29, 2006; In Final Form: February 14, 2007

New n-type conjugated oligomers bearing pyrenyl or triphenyl endgroups, 6,6′-bis(2-(1-pyrenyl)-4-phenylquinoline) (BPYPQ) and 6,6′-bis(2-(1-triphenyl)-4-phenylquinoline) (B3PPQ), were synthesized and found to be efficient blue emitters for organic light-emitting diodes (OLEDs). The oligoquinolines were thermally robust with high decomposition temperatures of 521−538 °C and high melt transitions (379−447 °C). The oligoquinolines emitted blue fluorescence in solution with high quantum yields (86−91%) and lifetimes of 1.31 ns for BPYPQ and 0.82 ns for B3PPQ. B3PPQ showed ambipolar redox properties, with a HOMO level of 5.78 eV and a LUMO level of 2.58 eV. BPYPQ had a reversible electrochemical reduction, with a HOMO level of 5.86 eV and a LUMO of 2.66 eV. Bright blue electroluminescence (3900 cd/m^2) with high efficiency (2.6 cd/A and 3.2% external quantum efficiency) were achieved from B3PPQ as the emitter in OLEDs. Far superior device performance was achieved with BPYPQ as the emissive material, with a maximum luminance of 13885 cd/m^2, an external quantum efficiency of 3.5% (at 5375 cd/m^2), and a luminous efficiency of 7.2 cd/A. The new triphenyl- and pyrenyl-bearing oligoquinolines are markedly thermally robust and are useful highly emissive and electron transport materials for OLEDs.

Introduction

Organic materials are finding increasing uses as light emitters and charge transporters in organic light-emitting diodes (OLEDs) for displays and lighting applications.[1−9] To fully realize the potential of these materials in organic electronics, improvement of device performance in terms of efficiency, stability, operational lifetime, brightness, and color purity requires a concomitant improvement in the active emissive/charge transport materials. Although a large number of small molecules, oligomers, and polymers have been investigated for applications in OLEDs, the vast majority of the synthetic effort, building blocks explored, and structure−property studies have been devoted to organic materials having dominant p-type (electron donor, hole transport) properties.[1−5] Our group[6d−f,7−9a,b] and others[6a−c,9c−f] have been interested in developing robust n-type organic semiconductors for applications in organic electronics, including quinoline-, quinoxaline-, anthrazoline-, pyrazinoquinoxaline-, and thienopyrazine-based materials.

Recently, we found that quinoline- and oligoquinoline-based donor−acceptor materials can have high fluorescence efficiency as thin films and lead to high-performance OLEDs of various colors.[7] An oligoquinoline with phenyl endgroups was found to be an efficient blue emitter and a good electron transport material for OLEDs.[7a] In contrast, a similar oligoquinoline with triphenylamine endgroups showed blue-green electroluminescence due to a strong intramolecular charge transfer interaction between the oligoquinoline acceptor and triphenylamine donor.[7c] To achieve new n-type emissive materials with pure blue emission while retaining the oligoquinoline core, it appears that suitable endgroups must be very weak electron donors or weak acceptors.[2e] Further, to improve the thermal stability the endgroups should be bulky aromatic groups.[7] Because excimer formation in organic semiconductors can dramatically red-shift the emission spectrum and substantially reduce the quantum yield,[10] and pyrene is well-known to readily form excimers in labeled flexible-chain polymers,[11] it would seem that pyrene is not a promising building block for developing emissive materials for OLEDs. However, there has been an increasing recent interest in the use of pyrenyl rings in the synthesis of emissive and charge transport materials for OLEDs,[5d,12−13] including oligothiophenes with pyrenyl side groups or endgroups,[5d] pyrene-triarylamine molecules,[12b] pyrenylamine-hexaphenylphenylene,[12c] pyrenyl-quinoxaline molecules,[13b] and pyrene-flourene derivatives.[13c]

In this paper we report the synthesis and investigation of new oligoquinolines with appended triphenyl or pyrenyl endgroups as light emitters and electron transport materials for OLEDs. The molecular structures of the n-type oligomers, 6,6′-bis(2-(1-pyrenyl)-4-phenylquinoline) (BPYPQ) and 6,6′-bis(2-(1-triphenyl)-4-phenylquinoline) (B3PPQ), are shown in Chart 1. The redox properties of the new oligomers were investigated by cyclic voltammetry, and related HOMO/LUMO levels were estimated. The photophysical properties of the new oligomers in solution and in thin films were investigated by steady state photoluminescence (PL) spectroscopy and by measuring the PL decay dynamics. The new oligomers were used as emitters in OLEDs and were found to exhibit high efficiency (3−7 cd/A, 3.4−3.5% external quantum efficiency) blue and blue-green electroluminescence.

Results and Discussion

Synthesis and Characterization. The synthesis of BPYPQ is shown in Scheme 1. 1-Acetylpyrene (**1**) was reacted with 5-bromo-2-aminobenzophenone (**2**) via Friedländer condensation to form the bromo-functionalized **3**. The monobromide **3** was

* E-mail: jenekhe@u.washington.edu.

10.1021/jp069037h CCC: $37.00
Published on Web 04/14/2007

CHART 1

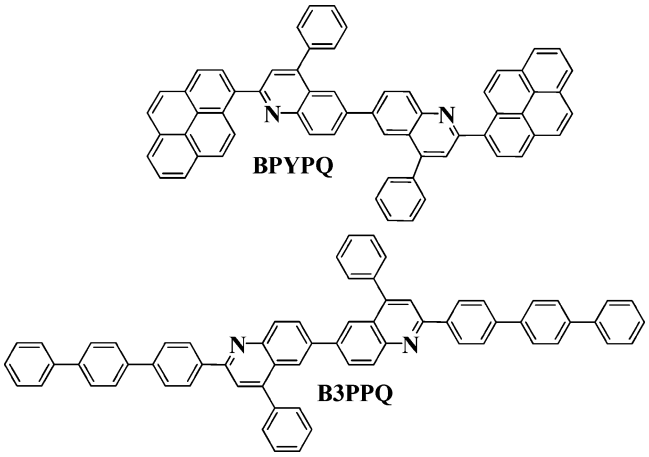

coupled under Stille conditions to form the target bis(2-(1-pyrenyl)-4-phenylquinoline) (BPYPQ) with a yield of 84%. Scheme 2 outlines the synthesis of B3PPQ. 4′-Bromoacetophenone (**4**) was reacted with 4-biphenylboronic acid (**5**) under Suzuki conditions to form 4-acetyl-triphenyl (**6**) in a 74% yield. The Friedländer condensation of **6** with 3,3′-dibenzoylbenzidine (**7**) gave the desired oligomer, 6,6′-bis(2-(1-triphenyl)-4-phenylquinoline (B3PPQ), with a yield of 85%. The structures of the oligomers were confirmed by mass spectrometry and ^{1}H NMR and FT−IR spectra.

The thermal transition characteristics and thermal stability of the oligomers were characterized by differential scanning calorimetry (DSC) and thermogravimetric analysis (TGA). Three distinct transitions were seen in the second-heating DSC scans of BPYPQ (Figure S1a): a clear T_g at 176 °C, an exothermic crystallization peak at 257 °C, and a melting peak (T_m) at 379 °C. We note that an exothermic peak was not observed in previous oligoquinolines that showed melt transitions.[7] It is reasonable to assume that the large aromatic pyrenyl endgroups tend to align and π-stack at temperatures above the T_g, resulting in a crystalline morphology. BPYPQ did not show a clear recrystallization peak upon cooling from the liquid phase. The second-heating DSC scan of B3PPQ revealed a T_m at 447 °C, but there was no clear glass transition (Figure S1b). The TGA of BPYPQ and B3PPQ showed high decomposition temperatures (T_D) of 538 °C and 521 °C, respectively. Evidently the addition of the bulky pyrenyl or triphenyl endgroups increases the thermal stability of the oligoquinoline, compared to previously studied oligoquinolines with smaller endgroups (T_D = 417−492 °C).[7] We also note that the glass transition, melting, and decomposition temperatures observed here are significantly higher than those previously reported for other materials containing pyrenyl moieties.[12−14] These thermally robust features of BPYPQ and B3PPQ are highly desirable for OLED applications.

Electrochemical Properties. The electronic states (HOMO/LUMO levels) of BPYPQ and B3PPQ were investigated by cyclic voltammetry (CV) to elucidate charge injection processes of the oligomers and the OLEDs based on them. The oxidation and reduction cyclic voltammograms of BPYPQ and B3PPQ thin films on platinum electrodes are shown in Figure 1. The oxidation CV of BPYPQ (Figure 1a) is characterized by an irreversible wave with a cathodic peak at +1.55 V (vs SCE). The onset oxidation potential (E_{ox}^{onset}) of BPYPQ is +1.46 V (vs SCE), similar to the irreversible oxidation potential of pyrene, +1.34 V (vs SCE).[14] The ionization potential (IP, HOMO level) of BPYPQ was estimated to be 5.86 eV from the onset oxidation potential by taking the SCE energy level to be −4.4 eV below the vacuum level (IP = E_{ox}^{onset} + 4.4).[15] B3PPQ showed a partially reversible oxidation wave (Figure 1c), with an onset potential of +1.38 V (vs SCE). The IP of B3PPQ, similarly calculated from the onset oxidation potential, is 5.78 eV.

The electrochemical reduction of BPYPQ and B3PPQ are shown in Figure 1b,d. The oligomers have reversible reduction waves that are nearly identical due to their identical oligoquinoline cores. The formal reduction potentials (E_{red}^{o}) of BPYPQ and B3PPQ are −1.87 V and −1.88 V (vs SCE), respectively. The onset of the first reduction wave is −1.74 V (vs SCE) for BPYPQ and −1.82 V (vs SCE) for B3PPQ. These values are very close to the reported reduction potential of bisphenylquinoline (2-PQ), which has an $E_{1/2}$ of −1.99 V.[16] This confirms that the major contribution to the LUMO level comes from the quinoline moieties of the oligomers. The estimated electron affinity (EA, LUMO level) values were calculated from the onset reduction potentials (EA = E_{red}^{onset} + 4.4). The EA is 2.66 eV for BPYPQ and 2.58 eV for B3PPQ. The electrochemical band gaps (E_g^{el}), estimated from IP-EA, are 3.2 eV for both BPYPQ and B3PPQ.

Photophysical Properties. The photophysical properties of BPYPQ and B3PPQ, including absorption maxima (λ_{max}^{abs}), molar absorption coefficients (ϵ), optical band gaps (E_g^{opt}), photoluminescence emission maxima (λ_{max}^{em}), fluorescence quantum yields (ϕ_f), excited state lifetimes, and Commission Internationale d'Eclairage (CIE) coordinates are summarized in Table 1. Figure 2 shows the normalized optical absorption and photoluminescence (PL) emission spectra of BPYPQ and B3PPQ in dilute ($5-7 \times 10^{-6}$ M) chloroform solutions and as thin films. The solution absorption spectrum of BPYPQ displays two bands at 286 nm (log ϵ = 4.91) and 380 nm (log ϵ = 4.91) and a shoulder at 344 nm (log ϵ = 4.75). B3PPQ exhibits two absorption peaks at 307 nm (log ϵ = 4.51) and 373 nm (log ϵ = 4.39) in chloroform solution. The absorption spectrum of thermally evaporated BPYPQ thin films has a similar structure to the solution state absorption with maxima at 277, 348, and 401 nm (Figure 2a). However, the peaks are broader, and the high-energy band is 1.5 times more intense in comparison to the solution state absorption. B3PPQ thin films have a high-energy absorption maximum of 308 nm and a $\pi-\pi^*$ transition band at 390 nm; this represents a 17 nm red-shift relative to solution. However, the red-shift of the $\pi-\pi^*$ band between solution and thin film was greater for BPYPQ (21 nm), indicating a greater increase in electron delocalization in the bulk solid state. In addition, the $\pi-\pi^*$ band in BPYPQ in both dilute solution and thin film is red-shifted by 7−11 nm compared to that of B3PPQ. This means that the extent of electron delocalization is greater with pyrene endgroups than with the triphenyl endgroups. This is further confirmed by the relatively high oscillator strength of the $\pi-\pi^*$ band in BPYPQ (log ϵ = 4.91) compared to that of B3PPQ (log ϵ = 4.39). The optical band gap (E_g^{opt}), calculated from the absorption band edge, is 2.7 eV for BPYPQ and 2.8 eV for B3PPQ. The optical band gap (E_g^{opt}) is 0.4−0.5 eV smaller than the 3.2 eV determined from electrochemistry. Such a difference between E_g^{opt} and E_g^{el} have been observed in conjugated polymers[15] and oligomers and arises from the finite binding energy of excitons in the material.[17]

The photoluminescence (PL) emission spectra of BPYPQ and B3PPQ are shown in Figure 2. In solution (chloroform), both oligomers emit intense blue fluorescence with CIE coordinates of (0.15, 0.07) and (0.16, 0.04) for BPYPQ and B3PPQ,

SCHEME 1: Synthesis of BPYPQ[a]

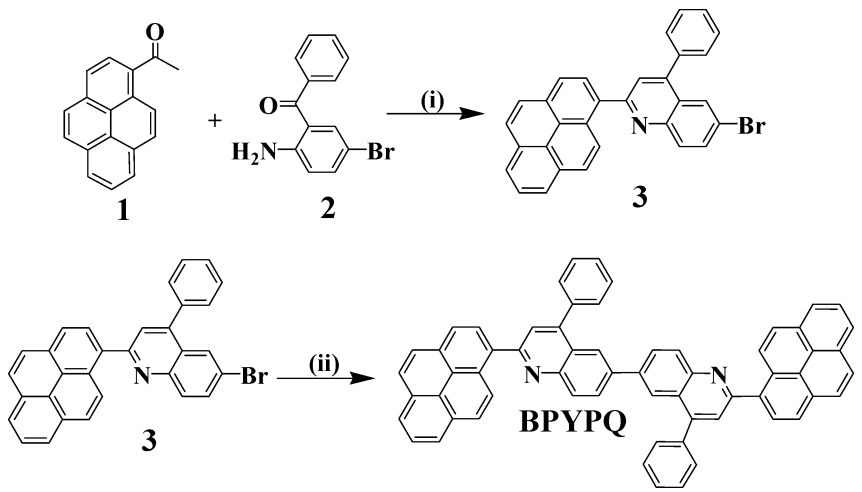

[a] Reagents and conditions: (i) diphenylphosphate, toluene, 120 °C, 24 h; (ii) $[Me_3Sn]_2$, $Pd[PPh_3]_4$, toluene, reflux 24 h.

SCHEME 2: Synthesis of B3PPQ[a]

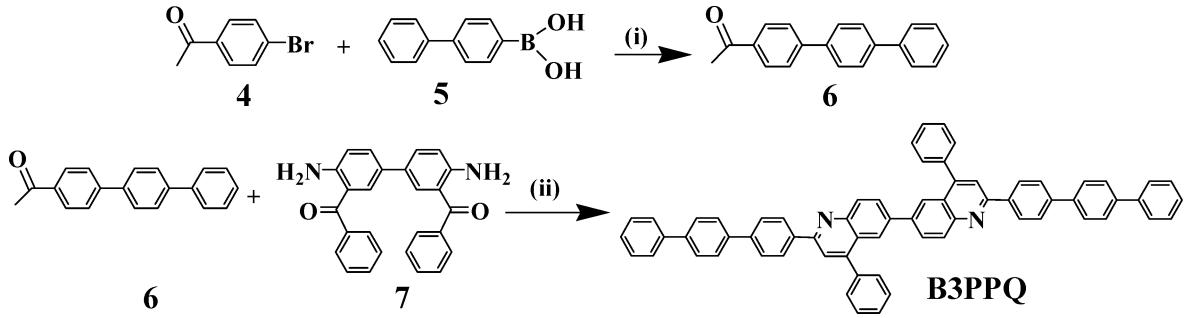

[a] Reagents and conditions: (i) 2 M Na_2CO_3, toluene, aliquot 86, reflux 24 h; (ii) DPP, toluene, 120 °C, 24 h.

respectively. The PL emission of BPYPQ is centered at 440 nm and has a full width at half-maximum (fwhm) value of 55 nm, with a quantum yield (ϕ_f) of 91%. B3PPQ in chloroform solution has a PL emission centered at 411 nm, a fwhm value of 48 nm, and a ϕ_f of 86%. The PL emission spectra of thin films of both compounds are also shown in Figure 2. The PL emission spectra of thin films of oligoquinolines are in general red-shifted from the solution spectra.[7] However, B3PPQ maintains its pure blue PL emission in the solid state with an emission maximum at 460 nm and CIE coordinates of (0.16, 0.18). In contrast, the solid state PL emission spectrum of BPYPQ is shifted into the green region with a band centered at 491 nm and CIE coordinates (0.19, 0.41). This red shift of the PL emission spectrum of BPYPQ relative to the solution spectrum is consistent with the observed red shift in the absorption spectrum when going from solution to thin film.

The PL decay dynamics of BPYPQ and B3PPQ were examined both in dilute solution and thin film to gain insight on the nature of the excited states responsible for efficient light emission. The PL decay curves of BPYPQ and B3PPQ are shown in the Supporting Information (Figures S2 and S3, respectively). In dilute chloroform solution ($5-7 \times 10^{-6}$ M), the PL decays of both BPYPQ and B3PPQ were well-described by single-exponential fits, and the goodness of the fit was characterized by χ^2 values of 1.5−1.6 and Durbin−Watson values of 1.34−1.35.[6e] BPYPQ had a PL lifetime (τ) of 1.31 ns whereas it was 0.82 ns in B3PPQ. These excited state lifetimes are consistent with expectations for singlet intramolecular excitons.[7] From the ϕ_{PL} value in solution and the excited state lifetime (τ) we estimate the radiative lifetime (τ_0) of the emission band to be 1.43 and 0.95 ns for BPYPQ and B3PPQ, respectively, according to $\phi_{PL} = \tau/\tau_0$.[7a,18]

As thin films, the PL decay was well-described by a biexponential fit for both BPYPQ and B3PPQ. BPYPQ exhibited a short lifetime component of 0.71 ns that dominated the emission with a relative amplitude of 86%, and a long lifetime component of 3.03 ns with a relative amplitude of 14%. With the measured lifetime (τ = 0.71 ns) of the PL emission of BPYPQ thin films, the ϕ_{PL} value of thin films was estimated to be ~50% ($\phi_{PL} = \tau/\tau_0$). B3PPQ had a short lifetime component of 0.54 ns (72%) and a longer lifetime component of 1.96 ns (28%), and it had an estimated thin film quantum yield of 57%. The biexponential fits had χ^2 values of 0.94−1.1 and Durbin−Watson values of 1.9−2.0. The short-lived species is attributed to intramolecular excitons, similar to the solution state excited state species. The origin of the minor long-lived species is not very clear. In polyquinoline thin films, long lifetimes on the order of 3−4 ns have been observed and were assigned to interchain excimers as a result of the favorable $\pi-\pi$ stacking interactions between the rigid planar polyquinoline chains.[8] Although pyrenyl rings are known to readily form excimers even in concentrated solution,[11] we rule out excimers in thin films of BPYPQ and B3PPQ in view of the relatively small Stokes shifts (70−90 nm) of their PL emission spectra, high PL quantum yield (50−57%) in BPYPQ and B3PPQ thin films, and comparable line shape of the solution and thin film spectra.

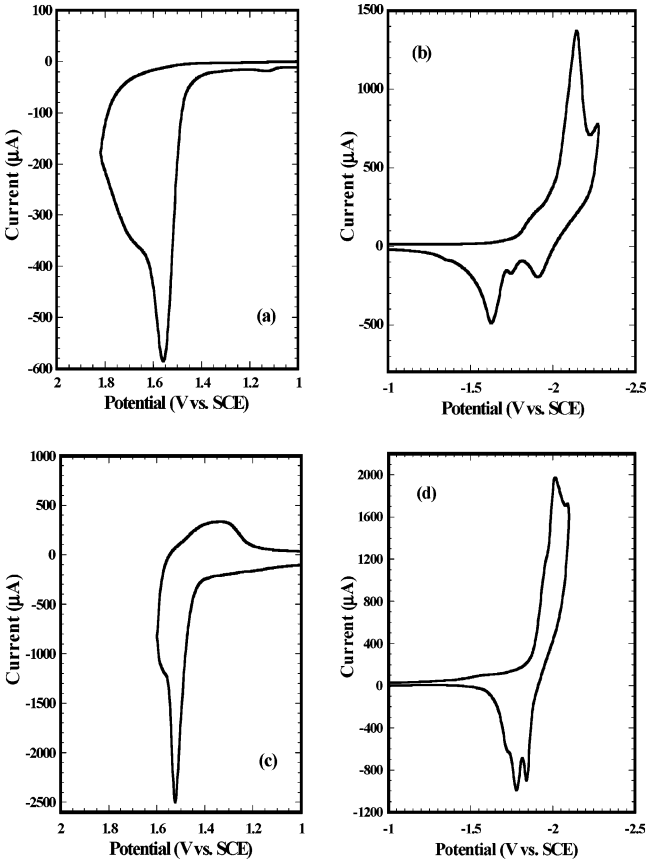

Figure 1. Cyclic voltammograms of the oxidation (a) and reduction (b) of BPYPQ and the oxidation (c) and reduction (d) of B3PPQ thin films on platinum wire; scan rate = 60 mV/s.

Electroluminescent Devices. OLEDs of different architectures were fabricated from the oligomers (BPYPQ and B3PPQ) and evaluated in ambient air. Five different device structures were investigated: ITO/oligomer/LiF/Al (diode I), ITO/PEDOT/PVK/oligomer/LiF/Al (diode II), ITO/PEDOT/PVK/oligomer/TPBI/LiF/Al (diode III), ITO/PEDOT/TAPC/oligomer/LiF/Al (diode IV), and ITO/PEDOT/TAPC/oligomer/TPBI/LiF/Al (diode V). The electroluminescent properties of all OLEDs, including turn-on voltage (V_{on}), drive voltage (V), maximum current density (mA/cm^2), luminance (cd/m^2), luminous efficiency (cd/A), external quantum efficiency (EQE), and electroluminescence (EL) emission maximum are summarized in Table 2. Single-layer OLEDs (diode I) had uniform electroluminescence, and the EL spectra of BPYPQ and B3PPQ were 5−12 nm blue-shifted from the corresponding thin film PL emission. The EL emission of BPYPQ was blue-green in color and had a maximum at 479 nm. B3PPQ emitted blue with an EL maximum at 455 nm. The performance of the single-layer devices (diode I) was poor for both BPYPQ and B3PPQ based diodes, obtaining brightnesses of 13−20 cd/m^2 and EQEs of 0.004−0.019%. This indicates inadequate charge carrier utilization in the single-layer diodes with most of the holes and electrons passing through the device with no recombination. As expected, the performance of these oligomers as emitters in OLEDs was greatly improved by using additional layers to facilitate the injection, transport, and confinement of electrons and holes (Table 2). An energy-level diagram showing all the HOMO and LUMO levels relevant to our OLEDs is shown in Figure 3. Devices using poly(*N*-vinylcarbazole) (PVK) (diode II) or 1,1-bis(4-tolylaminophenyl)cyclohexane (TAPC) (diode IV) as a hole-transport/electron-blocking layer (HTL) showed a turn-on voltage of 2.2−4.3 V at which uniform emission over the whole pixel was visible to the eye. For BPYPQ, the performance of diode II was superior to that of diode IV, implying that PVK (IP = 5.8 eV)[8a] is better at facilitating hole injection/transport while confining electrons to the emitter than TAPC (IP = 5.4 eV).[8a] Diode II based on BPYPQ, with a turn-on voltage of 3.7 V, had a maximum luminance of 14200 cd/m^2 (at 11.5 V) and maximum EQE of 1.7% at 5230 cd/m^2 and 3.3 cd/A. B3PPQ-based diodes exhibited far lower brightnesses, with the maximum luminance of 3900 cd/m^2 in diode IV (HTL = TAPC). Higher efficiencies for B3PPQ were achieved with PVK as the HTL with a 3.4% EQE at 210 cd/m^2 and 3.0 cd/A.

Diodes III and V incorporated 1,3,5-tris(*N*-phenylbenzimidizol-2-yl)benzene (TPBI, IP = 6.2−6.7 eV) as a hole-blocking layer (HBL) to confine holes within the emissive oligomer layer. The EL spectra for diodes III and V were identical to those of diodes I and II and were stable over the range of applied bias voltages (4−16 V). Representative EL spectra for BPYPQ and B3PPQ are shown in Figure 4. The EL emission spectra of diodes III and V were centered at 482−488 nm for BPYPQ and 458−461 nm for B3PPQ. The CIE coordinates of BPYPQ and B3PPQ electroluminescence are shown in Figure 5. BPYPQ diodes were blue-green in color with CIE coordinates of (0.18, 0.34) whereas B3PPQ diodes emitted pure blue with CIE coordinates of (0.18, 0.21).

The luminance−current density−voltage characteristics of diodes III and V for BPYPQ and B3PPQ are shown in Figure 6. The efficiencies of OLEDs employing BPYPQ as the emitter and PVK as the hole transport layer were enhanced more than 2-fold by the introduction of the TPBI layer, reaching efficiencies of 3.5% EQE and 7.2 cd/A at 5375 cd/m^2, and brightnesses of up to 13885 cd/m^2 (at 12.2 V). No significant enhancement was achieved in diode V, further demonstrating the superiority of PVK as the hole-transport layer in BPYPQ-based devices; this can be attributed to the lower charge injection barrier from PVK to BPYPQ compared to hole injection from TAPC to BPYPQ (Figure 3). The efficient hole injection in diode III results in poor charge balance, with holes passing through the BPYPQ layer. However, the addition of TPBI confines the holes within the BPYPQ layer resulting in an improved recombination rate. The addition of a TPBI layer did not enhance the efficiency of devices based on B3PPQ (Table 2). The lack of enhanced device performance indicates that B3PPQ has more balanced charge injection/transport, which is confirmed by its ambipolar redox properties, and that the charge recombination zone is within the oligomer layer. Additional evidence of this is the better single-layer device performance of B3PPQ relative to BPYPQ; a higher brightness was achieved at half the current density resulting in a 2.5-fold advantage in device efficiency in B3PPQ-based diodes (Table 2). The superiority of BPYPQ as an emitter was demonstrated in diode II−V. Diodes II−V exhibited as much as a 6.5-fold enhancement in brightness and diode III had a 1.5−3 fold increase in efficiency relative to B3PPQ based devices.

The variation in the luminous and power efficiency of diode III based on BPYPQ and B3PPQ are shown in Figure 7. The addition of TPBI introduces remarkable device efficiency stability for BPYPQ, where luminous efficiencies of ∼7 cd/A and power efficiencies of ∼1.8−2.0 lm/W are maintained over a wide range of luminances (up to 13500 cd/m^2) (Figure 7a). These results suggest balanced charge injection and recombination efficiency over the entire operating voltage range. In contrast, B3PPQ reaches maximum efficiencies of 2.5 cd/A (218 cd/m^2) and 0.69 lm/W (116 cd/m^2) whereupon the efficiencies

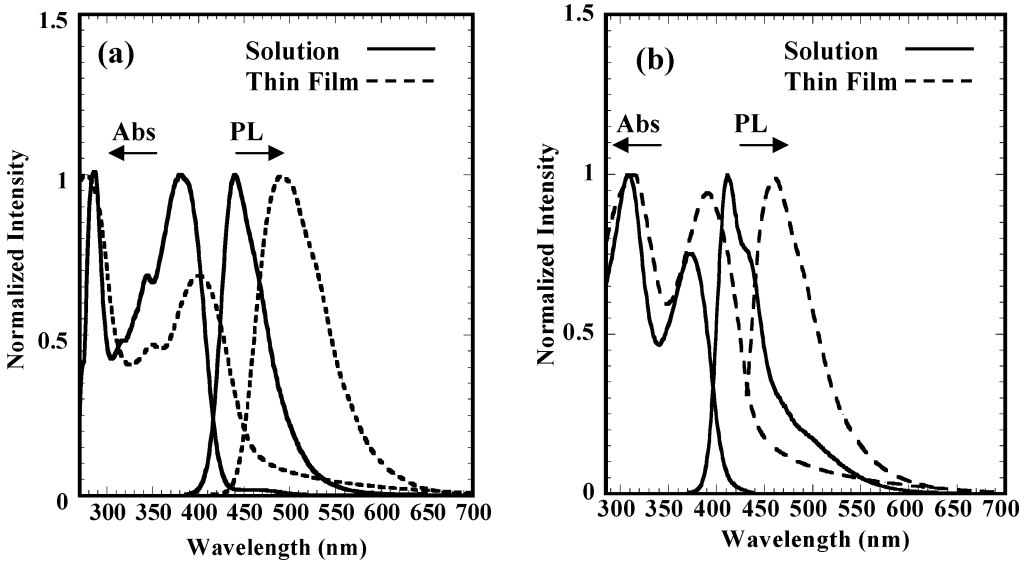

Figure 2. Normalized optical absorption and PL emission spectra of BPYPQ (a) and B3PPQ (b) in chloroform and as thin films.

TABLE 1: Photophysical Properties of Oligoquinolines BPYPQ and B3PPQ

oligomer		λ_{max}^{abs} (nm)	log ϵ	E_g^{opt} (eV)	λ_{max}^{em} (nm)	ϕ_f	τ (ns)	CIE (x, y)
BPYPQ	$CHCl_3$	286, 344, 380	4.91, 4.75, 4.91		440	0.91	1.31	(0.15, 0.06)
	thin film	277, 348, 401		2.7	491	0.50	0.71, 3.03	(0.19, 0.41)
B3PPQ	$CHCl_3$	307, 373	4.51, 4.39		411	0.86	0.82	(0.16, 0.04)
	thin film	308, 390		2.8	460	0.57	0.54, 1.96	(0.16, 0.18)

TABLE 2: Diode Characteristics of OLEDs Based on Oligomers BPYPQ and B3PPQ[a]

oligomer	diode[b]	V_{on}[c]	drive voltage (V)	current density (mA/cm^2)	luminance (cd/m^2)	diode efficiency (cd/A, %EQE[d])	λ_{max}^{EL} (nm)
BPYPQ	I	3.0	8.8	218	13	0.006, 0.004	479
	II	3.7	11.5	500	14200	2.3, 1.2	481
			11.2	*377*	*8348*	*3.3, 1.7*	
	III	4.2	12.2	238	13885	5.8, 2.8	482
			11.3	*75*	*5375*	*7.2, 3.5*	
	IV	2.2	8.7	500	11950	2.4, 1.0	480
			8.4	*370*	*8995*	*2.4, 1.1*	
	V	2.0	8.9	500	9947	2.0, 0.89	488
			6.5	*33*	*812*	*2.4, 1.1*	
B3PPQ	I	2.0	6.7	134	20	0.016, 0.019	455
	II	4.3	15.4	395	2200	0.56, 0.63	442
			10.1	*6.9*	*210*	*3.0, 3.4*	
	III	5.2	16.1	380	2780	0.73, 0.82	458
			11.8	*8.7*	*218*	*2.5, 2.8*	
	IV	3.5	8.3	346	3900	1.1, 1.4	449
			5.1	*12*	*336*	*2.6, 3.2*	
	V	3.3	12.5	414	4640	1.1, 1.4	461
			9.7	*32*	*567*	*1.8, 2.2*	

[a] Values in italic correspond to those for maximum device efficiencies. [b] Diode I: ITO/oligomer/LiF/Al. Diode II: ITO/PEDOT/PVK/oligomer/LiF/Al. Diode III: ITO/PEDOT/PVK/oligomer/TPBI/LiF/Al. Diode IV: ITO/PEDOT/TAPC/oligomer/LiF/Al. Diode V: ITO/PEDOT/TAPC/oligomer/TPBI/LiF/Al. [c] Turn-on voltage (at which EL is visible to the eyes). [d] EQE = external quantum efficiency.

steadily decrease with increased brightness, current density and applied voltage (Figure 7b).

Conclusions

We have synthesized and characterized two new n-type oligomers with oligoquinoline cores and pyrenyl or triphenyl endgroups, BPYPQ and B3PPQ, and found them to be thermally robust, efficient blue emitters and good electron transport materials for OLEDs. The oligomers BPYPQ and B3PPQ have high fluorescence quantum yields (86−91%). Bright (up to 13885 cd/m^2) and efficient (7.2 cd/A and 3.5% EQE) blue-green OLEDs were realized from the BPYPQ emitter. B3PPQ had ambipolar redox properties and blue electroluminescence with a maximum brightness of 2780 cd/m^2 and maximum efficiencies of 2.5 cd/A and 2.8% EQE. These results demonstrate that oligoquinolines bearing pyrenyl and triphenyl endgroups are attractive for applications in blue OLEDs and that the pyrenyl ring is an attractive building block in combination with n-type moieties.

Experimental Section

Materials. 1-Acetylpyrene, 2-aminobenzophenone, 4′-bromoacetophenone, 4-biphenylboronic acid, tetrakis(triphenylphosphine)palladium(0), diphenylphosphate, and all other reagents were purchased from Aldrich and were used as received unless stated otherwise. 3,3′- Dibenzoylbenzidine and 5-bromo-2-

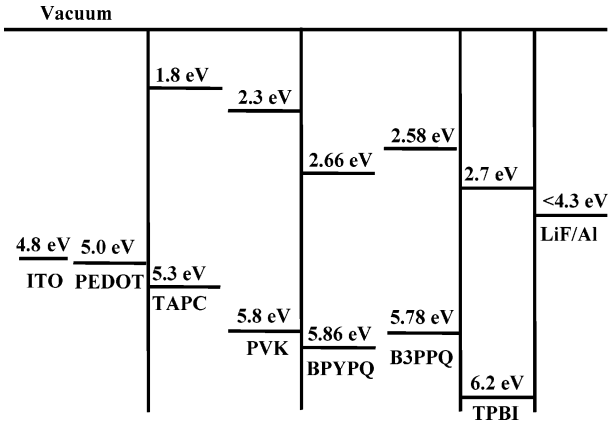

Figure 3. Energy levels (EA/IP) of the emissive oligomers (BPYPQ and B3PPQ) and hole or electron-blocking materials (TAPC, PVK, TPBI) used in the OLEDs.

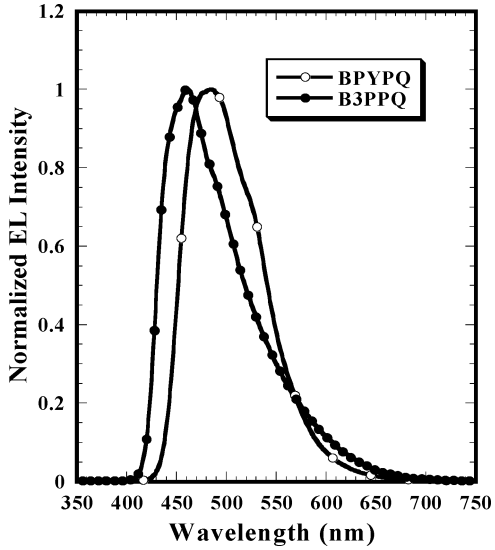

Figure 4. Normalized EL emission spectra of diode III based on BPYPQ and B3PPQ at 10 V.

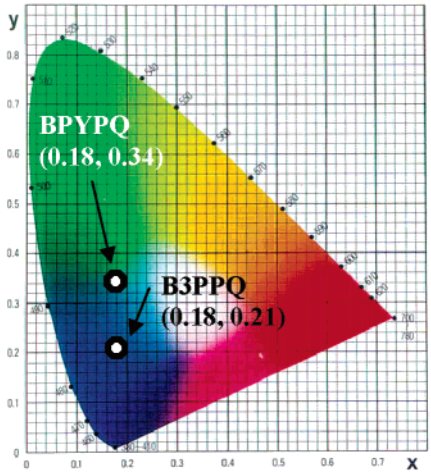

Figure 5. CIE coordinates of BPYPQ and B3PPQ electroluminescence (diode III) at 10 V.

aminobenzophenone were synthesized according to previous literature procedures.[19]

Synthetic Procedures. 2-(1-Pyrenyl)-4-phenyl-5-bromoquinoline (3). A total of 0.546 g (2.24 mmol) of 1-acetylpyrene (**1**), 0.515 g (1.87 mmol) of 5-bromo-2-aminobenzophenone (**2**), and 3 g of diphenyl phosphate (DPP) in 2 mL of toluene were stirred for 24 h at 120 °C under static argon. The reaction mixture was precipitated into 10% triethylamine/ethanol. The precipitate was collected by vacuum filtration, filtered through silica gel to remove polar byproducts, and then recrystallized twice from chloroform ($CHCl_3$). A total of 785 mg (87%) of yellow needles of **3** were recovered.

Bis(2-(1-pyrenyl)-4-phenylquinoline) (BPYPQ). A total of 0.641 g (1.32 mmol) of **3**, 0.22 g (0.67 mmol) of $[Me_3Sn]_2$, and 0.077 g (0.067 mmol) of $Pd[P(Ph)_3]_4$ were refluxed in anhydrous toluene overnight under argon. The resulting precipitate was collected via vacuum filtration and filtered through a silica gel column to remove tin byproducts. The product was recrystallized twice from $CHCl_3$ to yield 0.451 g (84%) of BPYPQ. Yield was 84% as light yellow crystals. T_m = 379 °C. ^{1}H NMR ($CDCl_3$): δ ppm = 8.61 (d, 2H), 8.48 (d, 2H), 8.38 (m, 6H), 8.26 (m, 4H), 8.18 (m, 8H), 8.07 (d, 2H), 7.91 (s, 2H), 7.72 (m, 4H), 7.61 (m, 6H). FT−IR (NaCl, cm^{-1}): 3046, 2922, 2339, 1586, 1572, 1549, 1536, 1477, 1425, 1364, 1232, 1157, 1121, 1049, 1031, 967, 884, 839, 828, 814, 782, 755, 720, 704. HRMS (FAB) calcd for $C_{62}H_{36}N_2$ 808.9916, found 809.2.

4-Acetyltriphenyl. A total of 50 mL of 2 M Na_2CO_3, 100 mL of toluene and 2 drops of Aliquot 86 were deaerated by bubbling argon through the mixture for 30 min while stirring. A total of 2.55 g (12.9 mmol) of 4-biphenylboronic acid, 2.88 g (14.5 mmol) of 4′-bromoacetophenone, and 0.250 g (0.216 mmol) of tetrakis(triphenylphosphine)palladium(0) were added and refluxed overnight. The organic layer was washed with water and dried with $MgSO_4$. The solvent was removed by rotoevaporation. The resulting product was filtered through a silica gel column and recrystallized from CH_2Cl_2/hexanes to give 2.60 g (9.55 mmol) as white crystals with a 74% yield.

6,6′-Bis(2-(1-triphenyl)-4-phenylquinoline) (B3PPQ). A total of 0.526 g (1.93 mmol) of 4-acetyl-triphenyl, 0.361 g (0.920 mmol) of 3,3′-dibenzoylbenzidine, and 2.5 g of diphenylphosphate in 2 mL of toluene were stirred for 24 h at 120 °C under static argon. The reaction mixture was precipitated into 10% triethylamine/ethanol. The solids were collected via vacuum filtration before being filtered through silica gel with $CHCl_3$ to remove impurities. The resulting off-white product was recrystallized in a large volume of $CHCl_3$ to give 0.677 g (0.783 mmol) as white crystals. Yield was 85% as small white crystals. T_m = 447 °C. ^{1}H NMR ($CDCl_3$): δ ppm = 8.55 (d, 2H), 8.44 (s, 2H), 8.36 (m, 6H), 8.27 (m, 4H), 7.72 (d, 2H), 7.60 (m, 8H), 7.45 (m, 20H). FT−IR (KBr, cm^{-1}): 3045, 3026, 2926, 2341, 1590, 1572, 1543, 1536, 1477, 1425, 1364, 1240, 1155, 1123, 1042, 1031, 967, 840, 828, 814, 755, 715, 706. HRMS (FAB) calcd for $C_{66}H_{44}N_2$ 865.1000, found 864.9.

Characterization. FT−IR spectra were taken on a Perkin-Elmer 1720 FTIR spectrophotometer with NaCl plates. ^{1}H NMR spectra were recorded on a Bruker-DRX499 at 500 MHz. Gel permeation chromatography (GPC) analysis of the oligomers was performed on a Waters gel permeation chromatograph with Shodex gel columns and Waters model 150 C refractive index detectors using THF as eluent and polystyrene standards. Differential scanning calorimetry (DSC) analysis was performed on a TA Instrument Q100 differential scanning calorimeter under N_2 at a heating rate of 10 °C/min, and thermogravimetric analysis (TGA) was conducted with a TA Instrument Q50 thermogravimetric analyzer at a heating rate of 10 °C/min under a nitrogen gas flow. UV−vis absorption spectra were recorded on a Perkin-Elmer model Lambda 900 UV/vis/near-IR spectrophotometer. The PL emission spectra were obtained with a Photon Technology International (PTI) Inc. model QM-2001-4

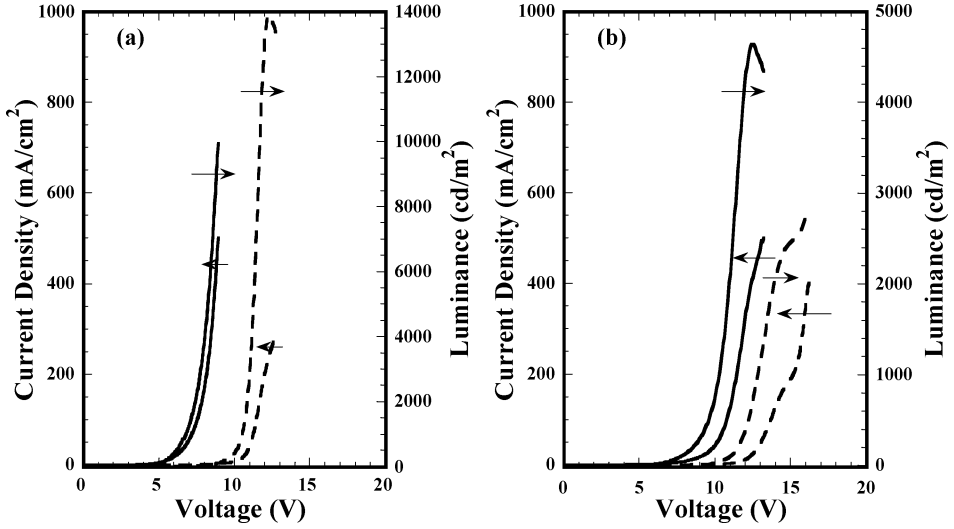

Figure 6. Luminance−current density−voltage characteristics of BPYPQ (a) and B3PPQ (b) devices; diode III (---) and diode V (—).

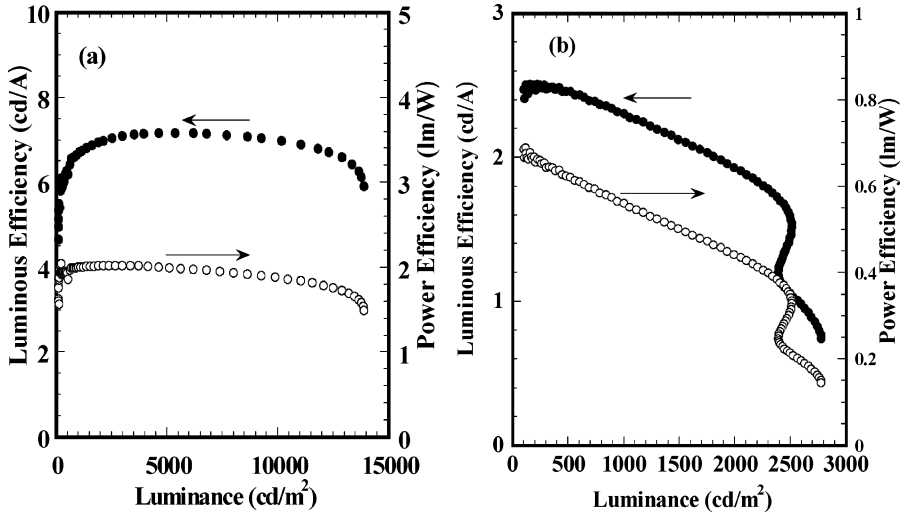

Figure 7. Luminous efficiency and power efficiency as a function of luminance (diode III) of BPYPQ (a) and B3PPQ (b).

spectrofluorimeter. To measure the PL quantum yields (ϕ_f), oligomer solutions in spectral grade toluene were prepared. The concentration ($\sim 10^{-6}$ M) was adjusted so that the absorbance of the solution was lower than 0.1. A 10^{-6} M solution of 9,-10-diphenylanthracene in toluene ($\phi_f = 0.93$) was used as a standard.[20]

Cyclic Voltammetry. Cyclic voltammetry experiments were done on an EG&G Princeton Applied Research Potentiostat/Galvanostat (Model 273A). Data were collected and analyzed on the Model 270 Electrochemical Analysis System software on a PC computer. A three-electrode cell was used in all experiments. Platinum wire electrodes were used as both counter and working electrodes, and silver/silver ion (Ag in 0.1 M $AgNO_3$ solution, Bioanalytical System, Inc.) was used as a reference electrode. The Ag/Ag^+ ($AgNO_3$) reference electrode was calibrated at the beginning of the experiments by running cyclic voltammetry on ferrocene as the internal standard in an identical cell without any oligomer on the working electrode. The films of the BPYPQ and B3PPQ were coated on the Pt working electrode by dipping the Pt wire into a viscous solution in formic acid and subsequently dried in a vacuum oven at 80 °C for 8 h. An electrolyte solution of 0.1 M $TBAPF_6$ in acetonitrile was used in the electrochemical cell. The solution was purged with ultrahigh purity N_2 for 10−15 min before the experiment, and a blanket of N_2 was used during the experiment. Electrochemistry was done at a scan rate of 60 mV/s. Solution CV measurements were not carried out due to the insolubility of BPYPQ and B3PPQ in polar organic solvents. Additionally, the oligomers were not soluble enough in benzene, diochloromethane, or dichlorobenzene to obtain 1 mM concentrated solutions to run CVs in mixed solvents.

Time-Resolved Photoluminescence Decay Dynamics. Fluorescence decays of the oligoquinolines in solution and as thin films were obtained on a PTI Model QM-2001-4 spectrofluorimeter equipped with a Strobe Lifetime upgrade. The instrument utilizes a nanosecond flash lamp filled with high-purity nitrogen/helium (30/70 v/v) mixture as the excitation source and a stroboscopic detection system. The decay curves were analyzed using a software package provided by the manufacturer. Reduced chi-square (χ^2) values, Durbin-Watson parameters, and weighted residuals were used as the goodness-of-fit criteria.[6e] All measurements were done in ambient conditions at room temperature.

Fabrication and Characterization of OLEDs. We fabricated OLEDs using BPYPQ and B3PPQ as the emitters and electron transport materials. Indium-tin oxide (ITO)-coated glass substrates (Delta Technologies Ltd., Stillwater, MN) were cleaned sequentially in ultrasonic baths of 2-propanol/deionized water (1:1 volume) mixture, toluene, deionized water, and acetone and then dried at 60 °C in vacuum overnight (~10 h). A 1 wt

% poly(ethylenedioxythiophene)/poly(styrene sulfonate) blend (PEDOT) dispersion in water was filtered through a 0.45 μm PVDF syringe filter. A 50 nm thick PEDOT layer was spin coated onto the ITO-coated glass to act as a hole injection layer and dried at 200 °C for 15 min under vacuum. A 15−20 nm thick hole-transport/electron-blocking later (HTL) was spin coated from its 1 wt % toluene solution onto the PEDOT layer and dried at 60 °C for 4 h under vacuum. A 40−50 nm thick film of each oligomer was evaporated from resistively heated quartz crucibles at a rate of 0.2−0.4 nm/s in a vacuum evaporator (Edwards Auto 306) at a base pressure of $<3 \times 10^{-6}$ Torr onto the HTL layer. Subsequently, a 15−20 nm thick hole blocking layer (TPBI) was evaporated onto the oligoquinoline layer. The chamber was vented with air to load the cathode materials, pumped down to $\sim 3 \times 10^{-6}$ Torr, and a 2 nm thick lithium fluoride layer followed by a 120 nm thick aluminum layer were deposited through a shadow mask to form active diode areas of 0.2 cm^2. The film thicknesses were measured by using an Alpha-Step 500 surface profiler (KLA Tencor, Mountain View, CA). Electroluminescence spectra were obtained using a PTI QM-2001-4 spectrophotometer. Current−voltage characteristics of the OLEDs were measured using a HP4155A semiconductor parameter analyzer (Yokogawa Hewlett-Packard, Tokyo). The luminance was simultaneously measured using a model 370 optometer (UDT instruments, Baltamore, MD) equipped with a calibrated luminance sensor head (model 211) and a 5× objective lens. The device external quantum efficiencies were calculated using procedures reported previously.[21] All the device fabrication and characterization steps were done under ambient laboratory conditions.

Acknowledgment. This research was supported by NSF STC-MDITR (DMR-0120967) at the University of Washington, the NSF (CTS-0437912), an NSF IGERT Nanotechnology Fellowship Award to J.M.H. from the Center of Nanotechnology, and in part by the Air Force Office of Scientific Research (Grant F49620-03-1-0162).

Supporting Information Available: Second heating DSC thermograms and PL decay curves of BPYPQ and B3PPQ. This material is available free of charge via the Internet at http://pubs.acs.org.

References and Notes

(1) See the special issue on organic electronics: *Chem. Mater*. **2004**, *16*, 4381−4846.

(2) (a) Tang, C. W.; VanSlyke, S. A. *Appl. Phys. Lett.* **1987**, *51*, 913. (b) Mitschke, U.; Bauerle, P. *J. Mater. Chem.* **2000**, *10*, 1471. (c) Chen, C. T. *Chem. Mater.* **2004**, *16*, 4389. (d) Shirota, Y. *J. Mater. Chem.* **2000**, *10*, 1. (e) Kulkarni, A. P.; Kong, X.; Jenekhe, S. A. *Adv. Funct. Mater*. **2006**, *16*, 1057.

(3) (a) Friend, R. H.; Gymer, R. W.; Holmes, A. B.; Burroughs, J. H.; Marks, R. N.; Taliani, C.; Bradley, D. D. C.; Dos Santos, D. A.; Brédas, J. L.; Lögdlund, M.; Salaneck, W. R. *Nature* **1999**, *397*, 121. (b) Kraft, A.; Grimsdale, A. C.; Holmes, A. B. *Angew. Chem., Int. Ed.* **1998**, *37*, 402. (c) Heeger, A. J. *Solid State Comm.* **1998**, *107*, 673. (d) Kulkarni, A. P.; Tonzola, C. J.; Babel, A.; Jenekhe, S. A. *Chem. Mater.* **2004**, *16*, 4556. (e) Yan, H.; Lee, P.; Armstrong, N. R.; Graham, A.; Evmenenko, G. A.; Dutta, P.; Marks, T. J. *J. Am. Chem. Soc.* **2005**, *127*, 3172. (f) Furuta, P. T.; Deng, L.; Garon, S.; Thompson, M. E.; Frechet, J. M. J. *J. Am. Chem. Soc.* **2004**, *126*, 15388. (g) Kulkarni, A. P.; Zhu, Y.; Jenekhe, S. A. *Macromolecules* **2005**, *38*, 1553. (h) Hughes, G.; Bryce, M. R. *J. Mater. Chem*. **2005**, *15*, 94.

(4) (a) *Electronic Materials: The Oligomer Approach*; Mullen, K., Wegner, G., Eds.; Wiley-VCH: Weinheim, Germany, 1998. (b) Martin, R. E.; Diederich, F. *Angew. Chem., Int. Ed.* **1999**, *38*, 1350.

(5) (a) Barbarella, G.; Melucci, M.; Sotgiu, G. *Adv. Mater*. **2005**, *17*, 1581. (b) Perepichka, I. F.; Perepichka, D. F.; Meng, H.; Wudl, F. *Adv. Mater*. **2005**, *17*, 2281. (c) Facchetti, A.; Yoon, M. H.; Stern, C. L.; Hutchison, G. R.; Ratner, M. A.; Marks, T. J. *J. Am. Chem. Soc.* **2004**, *126*, 13480. (d) Otsubo, T.; Aso, Y.; Takimiya, K. *J. Mater. Chem.* **2002**, *12*, 2565. (e) Chi, C.; Wegner, G. *Macromol. Rapid Commun.* **2005**, *26*, 1532.

(6) (a) Economopoulos, S. P.; Andreopoulou, A. K.; Gregoriou, V. G.; Kallitsis, J. K. *Chem. Mater*. **2005**, *17*, 1063. (b) Leclerc, M. *J. Polym. Sci. Part A.* **2001**, *39*, 2867. (c) Geng, Y.; Chen, A. C. A.; Ou, J. J.; Chen, S. H.; Klubek, K.; Vaeth, K. M.; Tang, C. W. *Chem. Mater*. **2003**, *15*, 4352. (d) Kulkarni, A. P.; Kong, X.; Jenekhe, S. A. *Macromolecules* **2006**, *39*, 8699. (e) Kulkarni, A. P.; Kong, X.; Jenekhe, S. A. *J. Phys. Chem. B.* **2004**, *108*, 8689. (f) Zhu, Y.; Yen, C. T.; Jenekhe, S. A.; Chen, W. C. *Macromol. Rapid Commun.* **2004**, *25*, 1829.

(7) (a) Kulkarni, A. P.; Gifford, A. P.; Tonzola, C. J.; Jenekhe, S. A. *Appl. Phys. Lett.* **2005**, *86*, 061106. (b) Shetty, A. S.; Liu, E. B.; Lachicotte, R. J.; Jenekhe, S. A. *Chem. Mater*. **1999**, *11*, 2292. (c) Hancock, J. M.; Gifford, A. P.; Zhu, Y.; Lou, Y.; Jenekhe, S. A. *Chem. Mater*. **2006**, *18*, 4924. (d) Tonzola, C. J.; Hancock, J. M.; Babel, A.; Jenekhe, S. A. *Chem. Commun.* **2005**, *41*, 5214. (e) Tonzola, C. J.; Kulkarni, A. P.; Gifford, A. P.; Kaminsky, W.; Jenekhe, S. A. *Adv. Funct. Mater*. **2007**, *17*, 863.

(8) (a) Zhang, X.; Shetty, A. S.; Jenekhe, S. A. *Macromolecules* **1999**, *32*, 7422. (b) Zhang, X.; Jenekhe, S. A. *Macromolecules* **2000**, *33*, 2069. (c) Zhu, Y.; Alam, M. M.; Jenekhe, S. A. *Macromolecules* **2003**, *36*, 8958. (d) Jenekhe, S. A.; Zhang, X.; Chen, X. L.; Choong, V.-E.; Gao, Y.; Hsieh, B. R. *Chem. Mater*. **1997**, *9*, 409. (e) Tonzola, C. J.; Alam, M. M.; Jenekhe, S. A. *Adv. Mater.* **2002**, *14*, 1086. (f) Tonzola, C. J.; Alam, M. M.; Jenekhe, S. A. *Macromolecules* **2005**, *38*, 9539.

(9) (a) Zhu, Y.; Champion, R. D.; Jenekhe, S. A. *Macromolecules* **2006**, *39*, 8712. (b) Cui, Y.; Zhang, X.; Jenekhe, S. A. *Macromolecules* **1999**, *32*, 3824. (c) Yamamoto, T.; Sugiyama, K.; Kushida, T.; Inoue, T.; Kanbara, T. *J. Am. Chem. Soc.* **1996**, *118*, 3930. (d) O'Brien, D.; Weaver, M. S.; Lidzey, D. G.; Bradley, D. D. C. *Appl. Phys. Lett.* **1996**, *69*, 881. (e) Jung, S.-H.; Kim, D. Y.; Cho, H.-N.; Suh, D. H. *J. Polym. Sci. A. Polym. Chem.* **2006**, *44*, 1189. (f) Huang, B.; Li, J.; Jiang, Z.; Qin, J.; Yu, G.; Liu, Y. *Macromolecules* **2005**, *38*, 6915.

(10) Jenekhe, S. A.; Osaheni, J. A. *Science* **1994**, *265*, 765.

(11) Winnik, F. M. *Chem. Rev.* **1993**, *93*, 587.

(12) (a) Jia, W.-L.; McCormick, T.; Liu, Q.-D.; Fukutani, H.; Motala, M.; Wang, R.-Y.; Tao, Y.; Wang, S. *J. Mater. Chem.* **2004**, *14*, 3344. (b) Justin Thomas, K. R.; Velusamy, M.; Lin, J. T.; Chuen, C. H.; Tao, Y.-T. *J. Mater. Chem.* **2005**, *15*, 4453.

(13) (a) Zhao, Z.; Zhang, P.; Wang, F.; Wang, Z.; Lu, P.; Tian, W. *Chem. Phys. Lett.* **2006**, *423*, 293. (b) Huang, T.-H.; Whang, W.-T.; Zheng, H.-G.; Lin, J. T. *J. Chin. Chem. Soc.* **2006**, *53*, 233. (c) Tang, C.; Liu, F.; Xia, Y.-J.; Xie, L.-H.; Wei, A.; Li, S.-B.; Fan, Q.-L.; Huang, W. *J. Mater. Chem.* **2006**, *16*, 4074. (d) Zhao, Z.; Xu, X.; Wang, F.; Yu, G.; Lu, P.; Liu, Y.; Zhu, D. *Synth. Met*. **2006**, *156*, 209.

(14) Ziessel, R.; Goze, C.; Ulrich, G.; Cesario, M.; Retailleau, P.; Harriman, A.; Rostron, J. P. *Chem. Euro. J.* **2005**, *11*, 7366.

(15) Agrawal, A. K.; Jenekhe, S. A. *Chem. Mater*. **1996**, *8*, 579.

(16) Lai, R. Y.; Fabrizio, E. F.; Lu, L.; Jenekhe, S. A.; Bard, A. J. *J. Am. Chem. Soc*. **2001**, *123*, 9112.

(17) Pope, M.; Swenberg, C. E. *Electronic Processes in Organic Crystals*, 2nd ed.; Oxford University Press: New York, 1999; p 841.

(18) Lakowicz, J. R. *Principles of Fluorescence Spectroscopy*; Plenum Press: New York, 1986; p 10.

(19) (a) Agrawal, A. K.; Jenekhe, S. A. *Macromolecules* **1993**, *26*, 895. (b) Tonzola, C. J.; Alam, M. M.; Bean, B. A.; Jenekhe, S. A. *Macromolecules* **2004**, *37*, 3554.

(20) Heinrich, G.; Schoof, S.; Gusten, H. *J. Photochem.* **1974**, *3*, 315.

(21) (a) Kulkarni, A. P.; Jenekhe, S. A. *Macromolecules* **2003**, *36*, 5285. (b) Okamoto, S.; Tanaka, K.; Izumi, Y.; Adachi, H.; Yamaji, T.; Suzuki, T. *Jpn. J. Appl. Phys.* **2001**, *40*, L783.